British Journal of Clinical Pharmacology

DOI:10.1111/bcp.12780

Investigating pulmonary and systemic pharmacokinetics of inhaled olodaterol in healthy volunteers using a population pharmacokinetic approach

Jens Markus Borghardt,[1,2] Benjamin Weber,[2] Alexander Staab,[2] Christina Kunz,[2] Stephan Formella[3] & Charlotte Kloft[1]

[1]Department of Clinical Pharmacy and Biochemistry, Institute of Pharmacy, Freie Universitaet Berlin, 12169 Berlin, Germany, [2]Translational Medicine and Clinical Pharmacology, Boehringer Ingelheim Pharma GmbH & Co. KG, Biberach, Germany and [3]Medicine Coordination, Boehringer Ingelheim Pharma GmbH & Co. KG, Ingelheim, Germany

Correspondence
Charlotte Kloft, Freie Universitaet Berlin, Institute of Pharmacy, Department of Clinical Pharmacy and Biochemistry, Kelchstr. 31, 12169 Berlin, Germany.
Tel.: +49 30 8385 0676
Fax: +49 30 8384 50656
E-mail: charlotte.kloft@fu-berlin.de

Keywords
inhalation, NONMEM, olodaterol, pharmacometrics, population pharmacokinetics, pulmonary absorption

Received
28 May 2015

Accepted
4 September 2015

Accepted Article Published Online
8 September 2015

WHAT IS ALREADY KNOWN ABOUT THIS SUBJECT

- Olodaterol is a long-acting β-adrenergic receptor agonist approved for the treatment of chronic obstructive pulmonary disease.
- The pulmonary absorption of dissolved drugs with similar physicochemical properties to olodaterol is widely considered as a fast process.

WHAT THIS STUDY ADDS

- This study is the first published pharmacokinetic analysis of plasma and urine data after intravenous administration and oral inhalation of olodaterol.
- A population pharmacokinetic approach demonstrated that olodaterol exhibits an extended pulmonary residence time (~22 h) for a large proportion of the pulmonary deposited dose (~70%) that was not expected from its physicochemical characteristics.

AIMS

Olodaterol, a novel β2-adrenergic receptor agonist, is a long-acting, once-daily inhaled bronchodilator approved for the treatment of chronic obstructive pulmonary disease. The aim of the present study was to describe the plasma and urine pharmacokinetics of olodaterol after intravenous administration and oral inhalation in healthy volunteers by population pharmacokinetic modelling and thereby to infer its pulmonary fate.

METHODS

Plasma and urine data after intravenous administration (0.5–25 μg) and oral inhalation (2.5–70 μg via the Respimat® inhaler) were available from a total of 148 healthy volunteers (single and multiple dosing). A stepwise model building approach was applied, using population pharmacokinetic modelling. Systemic disposition parameters were fixed to estimates obtained from intravenous data when modelling data after inhalation.

RESULTS

A pharmacokinetic model, including three depot compartments with associated parallel first-order absorption processes (pulmonary model) on top of a four-compartment body model (systemic disposition model), was found to describe the data the best. The dose reaching the lung (pulmonary bioavailable fraction) was estimated to be 49.4% [95% confidence interval (CI) 46.1, 52.7%] of the dose released from the device. A large proportion of the pulmonary bioavailable fraction [70.1% (95% CI 66.8, 73.3%)] was absorbed with a half-life of 21.8 h (95% CI 19.7, 24.4 h).

CONCLUSIONS

The plasma and urine pharmacokinetics of olodaterol after intravenous administration and oral inhalation in healthy volunteers were adequately described. The key finding was that a high proportion of the pulmonary bioavailable fraction had an extended pulmonary residence time. This finding was not expected based on the physicochemical properties of olodaterol.

Introduction

Chronic obstructive pulmonary disease (COPD) is one of the leading causes of death worldwide, creating both an economic and social burden [1, 2]. COPD is characterized by small airway obstructions and parenchymal destruction, causing persistent airflow limitations and acute exacerbations [2]. Although there is currently no cure for COPD, acute and persistent disease symptoms alike are treatable with various inhaled drugs. Short-acting bronchodilators, corticosteroids and antibiotics are considered the gold standard for treating acute exacerbations, whereas long-acting bronchodilators are the first-line therapy to treat persistent disease characteristics and to prevent exacerbations [2].

Olodaterol, a novel β2-adrenergic receptor agonist, is a long-acting, once-daily administered bronchodilator that has recently been approved for the treatment of COPD in the EU, USA and several other countries [3, 4]. It is administered by inhalation via the Respimat® soft mist™ inhaler, with the aim of achieving high pulmonary and, at the same time, low systemic concentrations. It is thereby possible to minimize the probability of systemic adverse events while still inducing a relaxation of pulmonary smooth muscle cells and thus maintaining efficacy [5–7]. Although it is generally accepted that delivering drugs directly to the lungs by inhalation results in a more favourable efficacy to systemic safety ratio compared with oral or intravenous (IV) administration [8], a quantitative and/or mechanistic understanding of the pulmonary fate [pulmonary pharmacokinetics (PK), including drug deposition] of inhaled drug is often lacking [9–11]. The benefits of an increased mechanistic understanding of the pulmonary fate of inhaled drugs include the possibility of improved treatment options for respiratory diseases, including COPD – for instance, to develop novel inhalation therapies (e.g. new drug compounds or new inhalation devices) with an optimized pulmonary concentration–time profile at the specific site of action (e.g. local areas of the lung).

Options for obtaining pulmonary tissue concentrations are currently limited, and are invasive. Studying pulmonary PK in isolated, perfused lung experiments can generate valuable information [12]. However, the time frame over which pulmonary PK can be studied in these experiments is often limited to a few hours and hardly suffices to capture pulmonary PK over several days [12], which may be an important aspect for drugs with a long pulmonary residence time. With the emerging science of modelling and simulation, new approaches for extracting information about the pulmonary fate of inhaled substances from human plasma PK studies have recently been proposed and successfully implemented [13]. Building on PK data obtained after IV administration and inhalation, these model-based approaches have demonstrated parallel absorption processes and extended pulmonary residence times for inhaled glycopyrronium and tiotropium, and thus helped increase the understanding of the pulmonary fate of these two compounds [13, 14]. Whether these findings are substance specific or can be generalized is currently of high interest.

Hence, the objective of the present analysis was to investigate the (pulmonary) PK of inhaled olodaterol by applying a nonlinear mixed-effects modelling approach (population PK approach) to plasma and urine data after IV administration and oral inhalation. Investigating the pulmonary fate of inhaled olodaterol, the population PK analysis also allowed studying the potential effects of subject characteristics (covariates) on pulmonary processes. Finally, the developed PK model was used for simulating the pulmonary and systemic PK profiles after single- and multiple-dose inhalations, with the aim of understanding how the PK processes might contribute to the rationale of once-daily dosing for olodaterol.

Materials and methods

Data for model development

Plasma and urine data from three Phase I clinical trials in healthy volunteers after IV infusion (single dose) and oral inhalation (single and multiple doses) of olodaterol were available for PK model development and evaluation. Oral data were not analysed as previous analyses of an absorption, distribution, metabolism and excretion (ADME) trial demonstrated that olodaterol has a negligible systemic availability after oral dosing [15]. Details on trial design, plasma sampling times and urine collection intervals are provided below.

The IV trial (trial 1) was a randomized, single-blind, placebo-controlled trial in which healthy volunteers received single doses of 0.5 μg, 2.5 μg, 5 μg, 10 μg, 15 μg, 20 μg, or 25 μg via infusion. The duration of the infusion was 30 min for doses lower than 15 μg and 3 h for doses higher than 15 μg. For the 15 μg dose, the duration of the infusion was either 30 min or 3 h. When the duration of the infusion was 30 min, blood samples were taken at 15 min, 29 min, 40 min, 50 min, 1 h, 1 h 20 min, 2 h, 3 h, 4 h, 6 h, 8 h, 10 h, 12 h, 24 h and 48 h (the 48-h sample was taken only for the 10 μg and 15 μg dosing groups) after the start of the infusion. Urine samples were collected at the following intervals after the start of the infusion: 0–4 h, 4–8 h, 8–12 h, 12–24 h, 24–48 h, 48–72 h and 72–96 h. When the duration of the infusion was 3 h, blood samples were taken at 3 min, 10 min, 30 min, 2 h 59 min, 3 h 3 min, 3 h 6 min, 3 h 10 min, 3 h 30 min, 4 h 30 min, 5 h 30 min, 6 h 30 min, 8 h 30 min, 10 h and 24 h after start of the infusion. Urine samples were collected at the following intervals after the start of the infusion: 0–4 h, 4–8 h, 8–12 h and 12–24 h.

The first inhalation trial (trial 2) was a randomized, double-blind, placebo-controlled single rising-dose trial, in which healthy volunteers inhaled doses of 2.5 μg, 5 μg, 10 μg, 15 μg, 20 μg, 30 μg, 40 μg, 50 μg, 60 μg, or 70 μg with the Respimat® inhaler. In addition, doses of 0.5 μg and 1 μg were administered but PK samples were not obtained. Depending on the dose group, blood samples were taken at 2 min, 5 min, 10 min, 20 min, 30 min, 40 min, 50 min, 1 h, 2 h, 3 h, 4 h, 6 h, 8 h, 10 h, 12 h, 24 h, 48 h, 72 h and 96 h after inhalation. Urine samples were collected at the following intervals after inhalation: 0–2 h, 2–4 h, 4–8 h, 8–12 h, 12–24 h, 24–48 h, 48–72 h, 72–96 h and 96–120 h.

The second inhalation trial (trial 3) was a randomized, double-blind, placebo-controlled trial in which healthy volunteers inhaled once-daily doses of 2.5 μg, 10 μg, or 30 μg with the Respimat® inhaler over 14 days. Extensive blood and urine sampling was performed after the first and the last (dose 14) inhaled dose. After the first inhaled dose, dependent on the dose group, blood samples were taken at 5 min, 10 min, 20 min, 30 min, 40 min, 1 h, 2 h, 4 h, 6 h, 8 h, 12 h and 24 h after inhalation. Urine samples were collected at the following intervals after inhalation: 0–4 h, 4–12 h and 12–24 h. After the last inhaled dose, depending on the dose group, blood samples were taken at 5 min, 10 min, 20 min, 30 min, 40 min, 1 h, 2 h, 4 h, 6 h, 8 h, 12 h, 24 h, 48 h, 72 h, 96 h, 168 h and 192 h after drug inhalation. Additional blood PK samples were taken on days 9, 12 and 13 (doses 10, 13 and 14) prior to drug inhalation. In contrast to urine sampling after single-dose inhalation, after the last inhaled dose (day 13, dose 14), urine samples were collected at the following intervals: 0–4 h, 4–12 h, 12–24 h, 24–48 h, 48–72 h, 72–96 h, 168–192 h and 216–240 h – i.e. in total over 10 days (days 13–23).

Blood samples were taken from a forearm vein in each subject and placed in EDTA coated collection tubes. Immediately after collection, the blood samples were centrifuged at 4–8 °C for 10 min at about 2000–4000 g. Both plasma and urine collections were stored at −20 °C or below until bioanalytical measurement. Urine and plasma concentrations were determined by validated high performance liquid chromatography–tandem mass spectrometry assays using [D_3]olodaterol as internal standard [16]. The lower limit of quantification was 2 pg ml^{-1} and 10 pg ml^{-1} for plasma and urine samples, respectively. In-study validation at three nominal concentrations demonstrated assay accuracy (relative deviation from target concentration) ranging from −7.7% to 8.5% for plasma and −3.5% to 5.5% for urine concentrations, precision (% CV) ranged from 0.2% to 9.4% for plasma and 2.1% to 8.2% for urine concentrations.

All trials were approved by the respective independent ethics committees [ethics committee of the local medical council in Mainz (trial 1 and trial 2), Medisch Ethische Toetsingscommissie Atrium Medisch Centrum – Maaslandziekenhuis (trial 3)] and were conducted in accordance with the Declaration of Helsinki and Good Clinical Practice guidelines. All healthy volunteers provided written informed consent before trial inclusion. More details can be found under the specific ClinicalTrials.gov identifier (trial 1: NCT02172131, trial 2: NCT02171780, trial 3: NCT02171806).

Model development

Model development was based on a stepwise approach that was previously described by Bartels *et al*. [13]. As a first step, plasma and urine measurements following IV administration were used to characterize the systemic distribution and elimination processes. This model is referred to as the 'systemic disposition model' below. As a second step, plasma and urine measurements following inhalation (trials 2 and 3) were used to characterize the combined PK of inhaled olodaterol (systemic disposition and upstream pulmonary PK processes, referred to as the 'combined PK model'). This second modelling step was performed under the assumption that the systemic disposition model was independent of the route of administration, meaning that the parameters of the systemic disposition model were fixed to the estimated values in the first step. Hence, in the second step only the pulmonary PK-related parameters (absorption rate constants and associated proportions absorbed by a specific absorption rate constant) were estimated. This additional part of the combined PK model is referred to as the 'pulmonary PK model'. Inclusion of olodaterol absorption from the gastrointestinal tract into the model was not necessary as the systemic availability of olodaterol after oral administration is virtually zero (based on data from an unpublished ADME trial). Data below the lower limit of quantification (LLOQ) were not included in the analysis.

Model development was performed using NONMEM 7.2 (Icon Development Solutions, Ellicott City, MD, USA).

Structural model In the first step of the model building process, different structural models, ranging from one- to five-compartment models, with drug clearance described by two linear clearance processes from the central compartment (renal and nonrenal), were investigated as systemic disposition models.

In the second step of the model building process, different structural pulmonary PK models were investigated: i) parallel first-order absorption processes, represented by depot compartments from which the drug was absorbed into the central compartment of the systemic disposition model; ii) parallel absorption processes, representing absorption into different compartments of the systemic disposition model; iii) parallel absorption processes with an additional pulmonary distribution compartment; and iv) parallel transit absorption models with absorption into the central compartment of the

systemic disposition model. A graphical representation of all investigated pulmonary absorption models can be found in the online Additional Supporting Information (Figure S1). The different structural pulmonary PK models were evaluated on top of the systemic disposition model developed in step one (model parameters were fixed to the estimates of the first step).

To describe the parallel absorption processes quantitatively, the total bioavailability was estimated, and assumed to represent the pulmonary bioavailable fraction of the dose released from the Respimat® inhaler (nominal dose). This assumption was based on the fact that olodaterol has a low systemic availability after oral dosing. In addition, each of the parallel absorption processes was characterized by two PK parameters: an estimated absorption rate constant and the respective proportion of the pulmonary bioavailable fraction absorbed. To calculate the different proportions of the pulmonary bioavailable fraction absorbed, proportionality parameters were estimated. The number of proportionality parameters was equal to the number of depot compartments representing pulmonary drug absorption minus one. For the transit absorption models, the transit rate constant was assumed to be equal for all transits and was estimated, along with the number of transit compartments. Both the pulmonary bioavailable fraction and the sum of all proportions of the pulmonary bioavailable fraction absorbed were constrained between zero and one.

A NONMEM control stream of the pulmonary PK model with parallel absorption processes is provided in Appendix S1, for better illustration of the principle of the proportionality parameters.

Random-effects model A forward inclusion approach was applied systematically to identify random-effect parameters. The first systemic disposition model included between-subject variability (BSV) of the nonrenal clearance. The first combined PK model included previously estimated BSV parameters of the systemic disposition model. Additional BSV parameters (variance and covariance parameters) were added to the models in a stepwise procedure until no additional improvement in model fit was observed; the parameter and their uncertainty estimation were still successful and the 95% confidence intervals did not include zero. BSV was assumed to be log-normally distributed.

If BSV was estimated on a structural parameter constrained between zero and one (i.e. pulmonary bioavailable fraction, proportionality parameters), BSV was assumed to be normally distributed and added to the logit-transformed parameter estimate. In a second step, the parameter associated with BSV was transformed using an inverse logit transformation, so that the resulting individual parameter estimate was again constrained between zero and one.

In a second step of the random-effects model development, between-occasion variability (BOV) was investigated for all pulmonary PK parameters associated with BSV. For model development, a combined residual variability model with two parameters, describing a proportional and an additive component, was used and reduced to a proportional residual variability model with only one parameter, if feasible [17]. The last step of model development (after covariate screening) was to re-evaluate variability parameters and remove them if the inclusion criteria were no longer fulfilled.

Covariate model A stepwise covariate modelling (SCM) approach including forward selection and backward elimination (alpha =0.05 and alpha =0.001) was used for identifying significant covariates for both the systemic disposition model and the pulmonary absorption model [Perl speaks NONMEM (PsN 4.2.0)] [18, 19]. Physiologic plausibility guided the selection of covariates to be tested. These comprised: the effect of body surface area (BSA); creatinine clearance; age; and smoking status on the clearance (nonrenal and renal), as well as the effect of BSA; gender; and age on both the volumes of distribution (V) and the between-compartment clearances (Q). Covariates assessed in the pulmonary absorption model comprised: the effect of smoking status and age on the absorption rate constants, as well as the effect of smoking status; age; gender; and BSA on the pulmonary bioavailable fraction and the proportionality parameters. As a further potentially important covariate, the administered dose was explored as a covariate on all PK parameters associated with BSV based on exploratory plots of individual random effects parameters stratified by dose. The covariate model for the systemic disposition model was developed based on IV data, whereas the covariate model for the pulmonary absorption model was developed based on inhalation data.

Decision criteria for model development Both graphical and numerical criteria were used for model evaluation and selection of a best PK model. Goodness-of-fit (GOF) plots included (individual) predictions *vs*. observations of olodaterol concentrations; individual PK profile plots; conditional weighted residuals *vs.* time (after dose); absolute individual weighted residuals *vs.* individual predictions; and density and quantile–quantile plots of BSV parameters. The numerical criteria included the decrease in the NONMEM objective function value; the precision of parameter estimates and the decrease in residual variability. Dose-normalized visual predictive checks (VPC) and VPCs to evaluate also plasma concentrations below the LLOQ [20] were performed to investigate the predictive performance of the key models (during model development) and the best model. Nonparametric bootstrapping was performed for the best PK model [18] to obtain nonparametric standard errors of the model parameter estimates (n = 200).

Simulations Monte-Carlo simulations (n = 1000) based on the best PK model (including BSV and BOV) were performed for once-daily drug inhalation for 10 days (5 μg, approved dose) to increase the understanding of the pulmonary and systemic PK processes of inhaled olodaterol. Simulation outcomes comprised the sum of drug amounts in all lung depot compartments; the sum of drug amounts in all systemic disposition compartments (body compartments); the plasma concentration; and the cumulative amount of drug excreted into the urine during one dose interval after multiple-dose inhalations (n = 10, assumption of steady-state attainment). Summary statistics, such as the areas under the curve (AUCs) for the different time profiles (drug amount in the depot compartments, drug amount in the body compartments, plasma concentration, cumulative amount excreted into the urine) after single drug inhalation (AUC_{0-24h}) and multiple drug inhalations ($AUC_{ss,\tau}$), were then calculated. In addition, drug accumulation was calculated based on either the previously determined AUCs or the simulated maximum plasma concentrations (C_{max}).

Results

Data

All three trials provided a total number of 148 healthy volunteers with PK data. Table 1 gives an overview of the characteristics of the data and the trial populations included in the analysis. Plasma concentration–time profiles and cumulative drug amounts eliminated into the urine are represented in Figure 1. Plasma concentrations after IV olodaterol administration (2.07–164 μg ml^{-1}) covered the range of plasma concentrations after olodaterol inhalation (2.00–72.1 μg ml^{-1}).

Model development

Structural model The systemic disposition model that best described the plasma and urine data after IV administration was a four-compartment model, with drug elimination described by two parallel first-order elimination processes from the central compartment (renal and nonrenal) (Figure 2, bottom). The combined PK model that best described the plasma and urine data after drug inhalation was characterized by three depot compartments, from which drug was absorbed into the central compartment of the disposition model with different first-order absorption rate constants (Figure 2, top = Figure S1, top middle).

Renal elimination of nonmetabolized olodaterol accounted for 14.2% of the total elimination. Thus, the nonrenal clearance was approximately sixfold higher than renal clearance. The pulmonary bioavailable fraction was estimated to be 49.4% of the nominal dose (ex-mouthpiece). The largest proportion (70.1%) of the pulmonary bioavailable fraction was absorbed slowly, with an absorption half-life of 21.8 h. The two remaining absorbed proportions

Table 1

Summary of trial and baseline demographic characteristics of healthy volunteers with pharmacokinetic (PK) data used for the population PK analysis

	Trial 1	Trial 2	Trial 3
Route of administration	IV	Inhalation	Inhalation
Dosing	Single	Single	Multiple
Administered doses with PK data (μg)	0.5–25	2.5–70	2.5–30
Number of healthy volunteers with PK data	48	65	35
Plasma PK data points above LLOQ used for analyses*	N = 435 TAD: 2 min to 24 h	N = 605 TAD: 2 min to 48 h 6 min	N = 547 TAD: 4 min to 96 h
Fraction of plasma PK data points below the LLOQ (%)	36.1	39.7	52.1
Urine PK data points above LLOQ used for analyses*	N = 231 TAD: 3 h 32 min to 96 h†	N = 440 TAD: 2 h to 96 h†	N = 396 TAD: 3 h 56 min to 240 h†
Fraction of urine PK data points below the LLOQ (%)	17.5	3.08	2.94
Gender (male/female; %)	100/0	90.8/9.2	74.3/25.7
Smoking status (nonsmoker/ex-smoker/smoker; %)	72.9/12.5/14.6	56.9/18.5/24.6	60.0/17.1/22.9
Age (median, range; years)	30.5 (22–43)	34 (22–49)	34 (22–48)
BSA (median, range; m^2)	1.96 (1.75–2.29)	1.98 (1.55–2.31)	2.02 (1.60–2.31)
Body weight (median, range; kg)	78 (65–101)	81 (54–105)	81 (53–103)
Body height (median, range; cm)	180 (168–194)	178 (157–192)	180 (162–194)
Creatinine clearance (median, range; ml/min)‡	121 (89–171)	116 (80–170)	117 (77–156)

*Small deviations of the time after dose compared with the data description in the text might be possible as these values represent the real sampling time points. †Time after dose for urine samples describes the time of the final urine collection of a specific urine collection time interval. ‡Creatinine clearance values were calculated according to the Cockcroft–Gault equation [45]. BSA, body surface area; IV, intravenous; LLOQ, lower limit of quantification; TAD, time after dose.

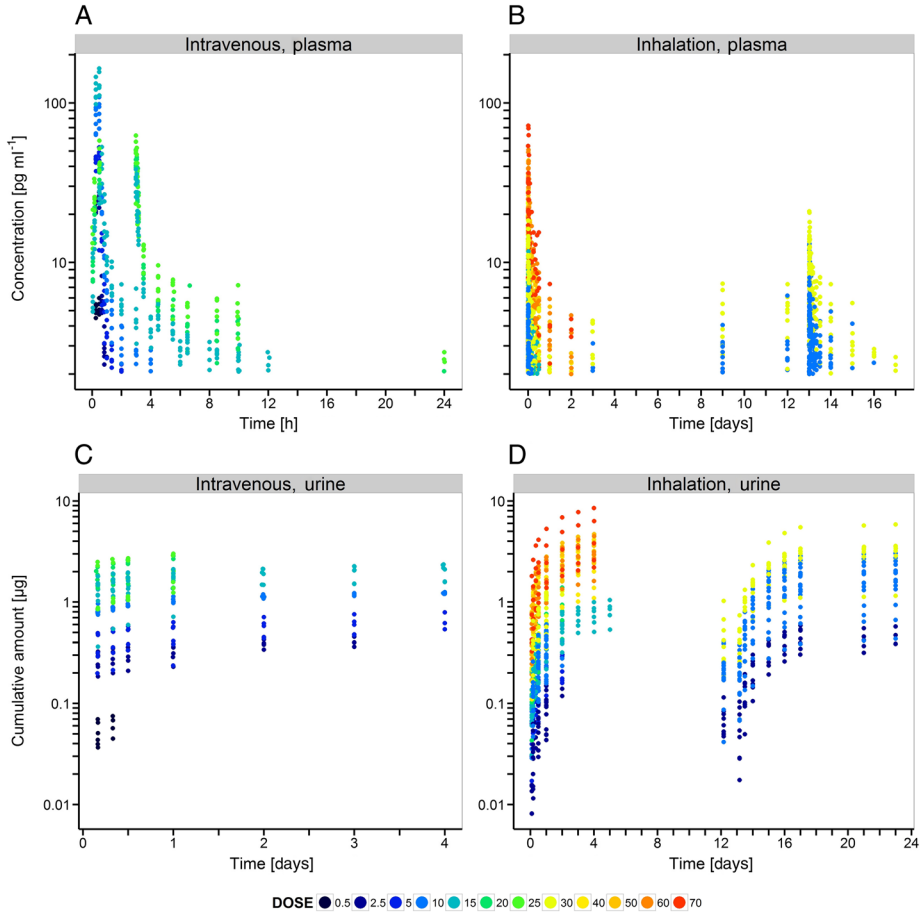

Figure 1

Semi-logarithmic plot of olodaterol plasma and urine data, including a colour grading for the different dosing regimens. (A) Plasma concentrations after intravenous administration (trial 1). (B) Plasma concentrations after oral inhalation (single and multiple rising-dose trials, trial 2 and trial 3). (C) Cumulative amount of drug excreted into the urine after intravenous administration (trial 1). (D) Cumulative amount of drug excreted into the urine after inhalation (single and multiple rising-dose trials, trial 2 and trial 3)

accounted for 26.6% and 3.32% of the pulmonary bioavailable fraction and were absorbed with absorption half-lives of 2.00 h and 0.268 h, respectively. The long terminal plasma half-life of 82.5 h after inhalation was identical to that after IV administration and, hence, was determined by the systemic disposition model and not by the slowest absorption process. A summary of all estimated model parameters, including relative standard errors of the estimates, is given in Table 2. Derived parameters calculated from the parameter estimates are given in Table 3.

Random-effects model BSV parameters for the systemic disposition model were estimated for the central volume of distribution (V_C), the intercompartmental clearances between the central and the first and second peripheral compartments (Q_2, Q_3), and the nonrenal clearance (CL_{NR}). For the combined PK model, additional BSV parameters were identified for the first and the second proportionality parameters (FF1, FF2). Additional covariances did not significantly improve the pulmonary absorption model. The variability of the pulmonary bioavailable fraction was better described by a BOV instead of a BSV parameter, so that the BSV was no longer necessary. No time dependent changes were observed for the pulmonary bioavailable fraction in the individuals. All parameters in the systemic disposition model and the combined PK model except V_2 were estimated with good precision (less than 20% relative standard error of the estimate; see Table 2). Point estimates of the parameters were in good agreement with results obtained from nonparametric bootstrapping, with deviations of less than 3% (relative to the point estimate), whereas the estimated standard errors of the PK parameters differed by less than 20% (absolute value). The highest η-shrinkage was 38.7% and 66.1% for BSV and BOV parameters, respectively, while the ε-shrinkage was low (6.83%).

GOF plots demonstrated the adequateness of the best PK model for both plasma (Figure 3) and urine (Figure 4) data for all investigated dosing regimens. The results of dose-normalized VPCs and VPCs to evaluate plasma concentrations below the LLOQ (Figure 5) were in agreement with the goodness-of-fit criteria (Figures 3 and 4) and

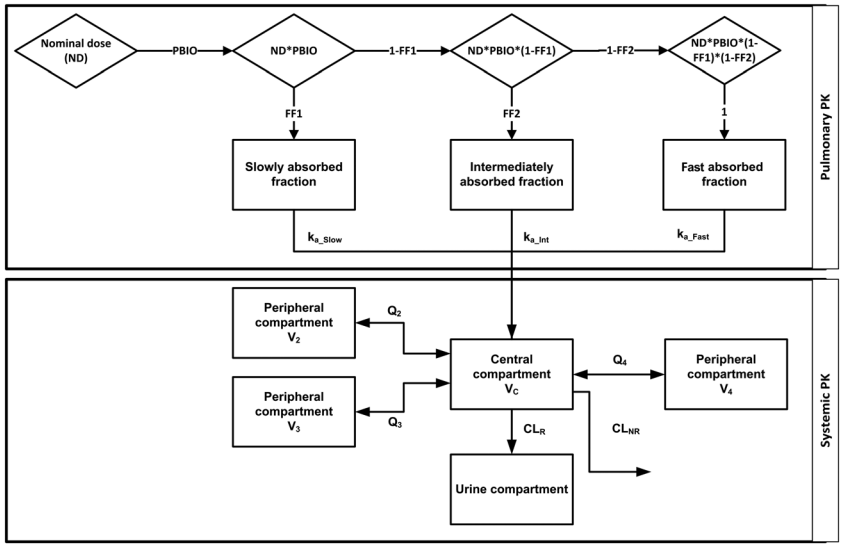

Figure 2

Schematic representation of the best pharmacokinetic (PK) model. Pulmonary PK box: Pulmonary PK model; systemic PK box: systemic disposition model; rhombus: calculated values; rectangles: model compartments; arrows from the absorption compartments to the central systemic compartment represent the absorption processes. CL_R, renal clearance; CL_{NR}, nonrenal clearance; FF1, first proportionality parameter; FF2, second proportionality parameter; k_{a_slow}, slow absorption rate constant; k_{a_int}, intermediate absorption rate constant; k_{a_fast}, fast absorption rate constant; ND, nominal dose (ex-mouthpiece); PBIO, pulmonary bioavailable fraction; Q_2–Q_4: inter-compartmental clearances; V_C–V_4, volumes of distribution. Whenever the next dose was inhaled, the calculation of the cumulative amount of drug excreted into the urine was restarted

Table 2

Estimated pharmacokinetic model parameters

Parameter	Abbreviation	Unit	Population estimate (% RSE)	BSV [% CV] (% RSE)
Central volume of distribution (CMT 1)*	V_C	[l]	23.5 (4.35)	26.2 (10.4)
Peripheral volume of distribution (CMT 2)*	V_2	[l]	2590 (35.7)	–
Peripheral volume of distribution (CMT 3)*	V_3	[l]	473 (10.7)	–
Peripheral volume of distribution (CMT 4)*	V_4	[l]	16.1 (19.7)	–
Inter-compartmental clearance (to CMT 2)*	Q_2	[l h^{-1}]	31.7 (12.3)	25.7 (13.5)
Inter-compartmental clearance (to CMT 3)*	Q_3	[l h^{-1}]	65.7 (5.28)	16.8 (13.5)
Inter-compartmental clearance (to CMT 4)*	Q_4	[l h^{-1}]	22.5 (8.06)	–
Renal clearance*	CL_R	[l h^{-1}]	10.5 (4.55)	–
Nonrenal clearance*	CL_{NR}	[l h^{-1}]	63.7 (8.49)	26.8 (13.5)
Slow absorption rate constant	k_{a_slow}	[h^{-1}]	0.0318 (5.23)	–
Intermediate absorption rate constant	k_{a_int}	[h^{-1}]	0.347 (7.04)	–
Fast absorption rate constant	k_{a_fast}	[h^{-1}]	2.59 (9.97)	–
Pulmonary bioavailable fraction	PBIO	[% ND]	49.4 (3.32)	BOV: 32.2 (8.50)†
First proportionality parameter	FF1	[%]	70.1 (2.33)	11.4 (14.0)
Second proportionality parameter	FF2	[%]	88.9 (1.89)	9.33 (16.0)
Impact of active smoking on k_{a_fast}	–	–	1.08 (18.0)	–
Impact of active smoking on k_{a_slow}	–	–	−0.380 (10.2)	–
Proportional residual variability (plasma)	–	[% CV]	15.8 (1.66)	–
Additive residual variability (plasma)	–	[pg ml^{-1}]	0.00001 fixed	–
Proportional residual variability (urine)	–	[% CV]	37.7 (2.30)	–
Additive residual variability (urine)	–	[pg ml^{-1}]	0.00001 fixed	–

*Parameters were estimated based on intravenous data. †BOV instead of BSV. BSV, between-subject variability; BOV, between-occasion variability; CV, coefficient of variation; ND, nominal dose (ex-mouthpiece); RSE, relative standard error.

Table 3

Derived pharmacokinetic (PK) model parameters

Parameter	Abbreviation	Units	Calculated value
Slow absorption half-life	$t_{1/2\_slow}$	[h]	21.8
Intermediate absorption half-life	$t_{1/2\_int}$	[h]	2.00
Fast absorption half-life	$t_{1/2\_fast}$	[h]	0.268
Slow absorption rate constant (smoker)	$k_{a\_slow\_smoker}$	[h^{-1}]	0.0197
Fast absorption rate constant (smoker)	$k_{a\_fast\_smoker}$	[h^{-1}]	5.39
Slow absorption half-life (smoker)	$t_{1/2\_slow\_smoker}$	[h]	35.2
Fast absorption half-life (smoker)	$t_{1/2\_fast\_smoker}$	[h]	0.129
Proportion of the pulmonary bioavailable fraction slowly absorbed	Fr_{slow}	[%]	70.1
Proportion of the pulmonary bioavailable fraction intermediately absorbed	Fr_{int}	[%]	26.6
Proportion of the pulmonary bioavailable fraction fast absorbed	Fr_{fast}	[%]	3.32
Bioavailability of slowly absorbed drug	F_{slow}	[% ND]	34.6
Bioavailability of intermediately absorbed drug	F_{int}	[% ND]	13.2
Bioavailability of fast absorbed drug	F_{fast}	[% ND]	1.64
Fraction excreted into the urine	F_e	[% of total elimination]	14.2

Calculated from the population PK parameter estimates in Table 2, with half-lives calculated using t½ = ln(2)/k. ND, nominal dose (ex-mouthpiece).

demonstrated an overall good predictive performance for both matrices (Figure 5).

Covariate model Based on IV data, no significant covariates were identified for the systemic disposition model. Based on oral inhalation data, smoking decreased the absorption half-life of the fast absorption process by 51.9%, to 0.129 h and increased the absorption half-life of the slow absorption process by 61.5%, to 35.2 h (both $P < 0.001$). There was no difference between ex-smokers and lifetime nonsmokers. The forward selection of the SCM approach also indicated that females had a higher pulmonary bioavailable fraction ($P < 0.05$); however, this covariate was removed during the backward elimination process ($P > 0.001$).

Simulations PK simulations were performed both for smokers and nonsmokers (Figure 6). The amount of drug in the pulmonary depot compartments was 55.8% higher at steady state ($AUC_{ss,\tau}$) for smokers compared with nonsmokers. This represented the largest difference between the two populations, indicating a higher pulmonary residence time of olodaterol in smokers. There was a less pronounced difference in the calculated $AUC_{ss,\tau}$ for the amount of drug in the body compartments, the plasma concentration–time profile and the cumulative amount of drug excreted into the urine after multiple dosing, with relative differences of less than 3% between smokers and nonsmokers. Differences between smokers and nonsmokers in three AUC_{0-24h} values (drug amount in the body compartments, plasma concentration and cumulative amount excreted into the urine) after single-dose inhalation were more pronounced (except for the AUC_{0-24h} for the amount of drug in the depot compartments, compared with steady state), ranging from 9% to 19%. Drug accumulation in the plasma, which was calculated based on AUC_{0-24h} and $AUC_{ss,\tau}$ for the plasma concentrations after single and multiple doses, was 2.67 and 2.15 for smokers and nonsmokers, respectively. Compared with these values, drug accumulation calculated with the simulated C_{max} was lower; i.e. 1.48 and 1.44 for smokers and nonsmokers, respectively. Drug accumulation in the body compartments was highest, with accumulation ratios of 8.30 and 7.05 in smokers and nonsmokers, respectively.

Discussion

A population PK model-based approach was applied to investigate the pulmonary fate of inhaled olodaterol and to identify patient factors influencing pulmonary and plasma PK after single and multiple doses of a broad range of doses administered IV and by inhalation. Absorption of swallowed drug after inhalation, was considered negligible based on a previous ADME trial. The PK model that best described the plasma and urinary concentrations incorporated three paralell pulmonary absorption processes. A key finding was that a large proportion of the pulmonary bioavailable fraction (approximately 70%) was slowly absorbed, with an absorption half-life of approximately 1 day. Pulmonary absorption half-lives of small molecules with log octanol–water partition coefficients similar to that of olodaterol (the log D value at pH 7.4 is 1.2 [21]) are generally assumed to be between 1 min and 1 h [22]. Hence, the finding that a large proportion of the pulmonary bioavailable fraction exhibits a prolonged pulmonary residence time does not agree with the general assumption that dissolved drug is being rapidly absorbed from the lung [9, 10]. However, it is consistent with a recent publication, in which a modelling approach demonstrated an extended residence time for a significant proportion of the pulmonary bioavailable fraction following tiotropium inhalation, which was administered in the form of a solution [14]. The slow absorption process contributed to drug accumulation after multiple drug inhalations. The fast and intermediate absorption processes were the main contributors to the early C_{max}

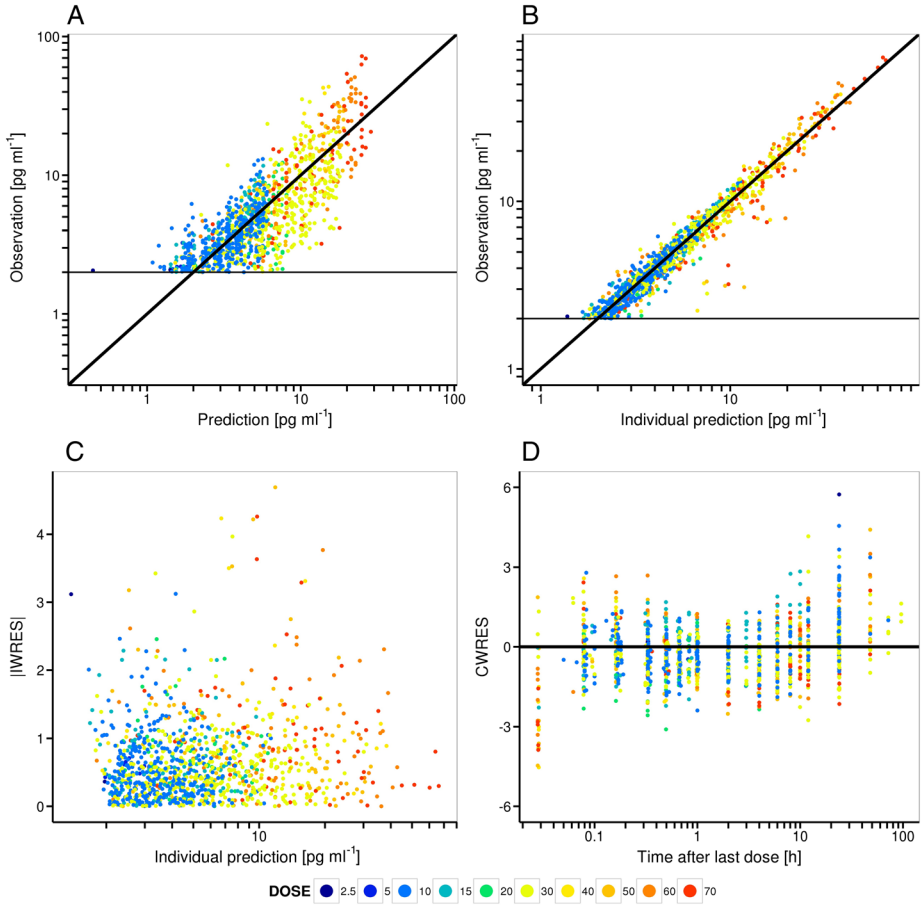

Figure 3

Standard goodness-of-fit plots for plasma pharmacokinetic (PK) data after olodaterol inhalation, including a colour grading for the different dosing regimens. (A) Logarithmic plot of olodaterol observations *vs*. predictions. (B) Logarithmic plot of observations *vs*. individual predictions. (C) Semi-logarithmic plot of absolute individual weighted residuals (IWRES) *vs*. individual predictions. (D) Semi-logarithmic plot of conditional weighted residuals (CWRES) *vs*. time after last dose. In (A) and (B), the thick black line represents the line of identity and the thin black line represents the lower limit of quantification. In (C) and (D), the thick black line represents the reference line

and the initial shape of the plasma concentration-time profile. The fast absorption half-life (~16 min) is in good agreement with the value predicted from the log D value.

The three parallel first-order absorption processes (slow, intermediate and fast) are in agreement with recent publications for orally inhaled glycopyrronium [13], tiotropium [14] and morphine [23]. Alternative pulmonary PK models that were investigated for inhaled olodaterol (e.g. transit absorption model, direct absorption into peripheral compartments; see Figure S1) could not be supported with the PK data.

The main route of elimination identified with the PK model was nonrenal clearance, consistent with a previous ADME trial. This pronounced nonrenal elimination results in negligible oral bioavailability and rapid elimination, ultimately contributing to low systemic adverse effects and efficient lung targeting after oral inhalation. For inhaled drugs, low oral bioavailability can be considered beneficial as the swallowed drug fraction after inhalation does not contribute to systemic adverse events. Low plasma concentrations due to a high systemic olodaterol clearance can additionally be considered to contribute to efficient targeting of the lungs after oral drug inhalation.

The random-effects model was consistent with previous findings for oral drug inhalation: A higher BOV compared with BSV was demonstrated [24]. This was thought to be the result of varying breathing patterns [25]. Variability in the pulmonary bioavailable fraction of olodaterol was also better described by a BOV than a BSV parameter. However, given the available PK data, it was difficult to distinguish between BOV and BSV. For individuals who contributed only single-dose data, BSV and BOV could not be differentiated and were combined into a single variability term. To better predict individual concentration-time profiles, additional data, such as individual inhalation flows should be included in the PK model development. Individual inhalation flows were not available in the clinical trials available for this analysis.

The inclusion of urine data in the analysis was critical for adequately characterizing model parameters. In the

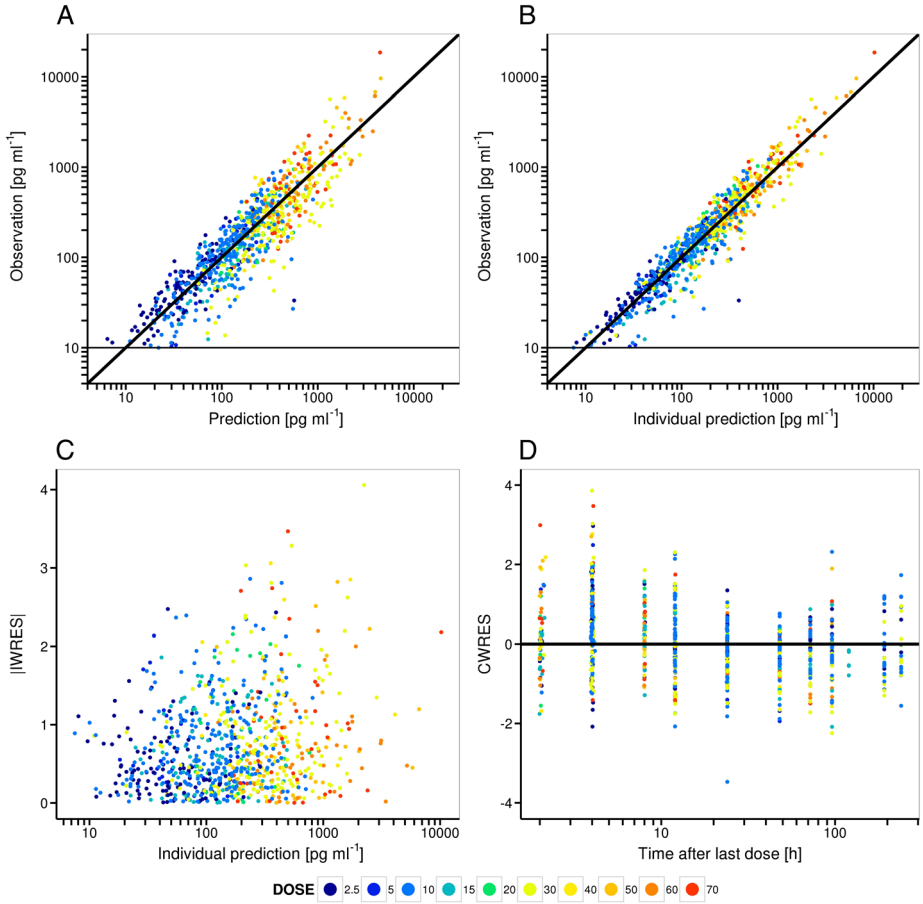

Figure 4

Standard goodness-of-fit plots for urine data after olodaterol inhalation, including a colour grading for the different dosing regimens. (A) Logarithmic plot of observations *vs.* predictions. (B) Logarithmic plot of observations *vs.* individual predictions. (C) Semi-logarithmic plot of absolute individual weighted residuals (IWRES) *vs.* individual predictions. (D) Semi-logarithmic plot of conditional weighted residuals (CWRES) *vs.* time after last dose. In (A) and (B), the thick black line represents the line of identity and the thin black line represents the lower limit of quantification; in (C) and (D), the black line represents the reference line

absence of the urine data, a three-compartment systemic disposition model was sufficient for describing IV plasma data [15]. The same qualitative results (three pulmonary absorption processes) were identified in the best pulmonary model. The slow pulmonary absorption process was the rate-limiting step that drove the terminal half-life and caused accumulation after multiple inhalations (effective half-lives [26] of 8.75 h and 34.0 h derived from the PK model after IV bolus administration and inhalation, respectively). After inclusion of the urine data in the PK analysis, a four compartment systemic disposition model was needed to characterize IV plasma and urine data adequately. The terminal half-life was 82.5 h after both IV administration and inhalation, indicating that it was independent of the absorption process. The effective half-lives [26] were 13.6 h and 29.0 h for IV bolus administration and inhalation, respectively. Thus, even though the terminal half-life was independent of the absorption process, drug accumulation after inhalation was still dependent on the pulmonary absorption process.

A previous analysis demonstrated that including data below the LLOQ in the model did not affect the systemic disposition model (results not shown here). Therefore, the impact of including urine data in model development was more pronounced than expected (see above). This may be due to the availability of urine data over a longer time period than plasma concentrations above the LLOQ.

Smoking was found be a significant covariate on the slow and fast pulmonary absorption rate constants. The effect of smoking on the fast absorption process is in agreement with previously published studies. These studies demonstrated that smoking inhibits tight junctions in the lung [27], resulting in faster drug absorption through the airway epithelia [28]. The formation of new tight junctions and a decrease in pulmonary epithelial permeability can be observed as soon as 24 h after the last smoking activity [29, 30]. This might explain why there was no significant difference between ex-smokers and nonsmokers in the present study. The same effect

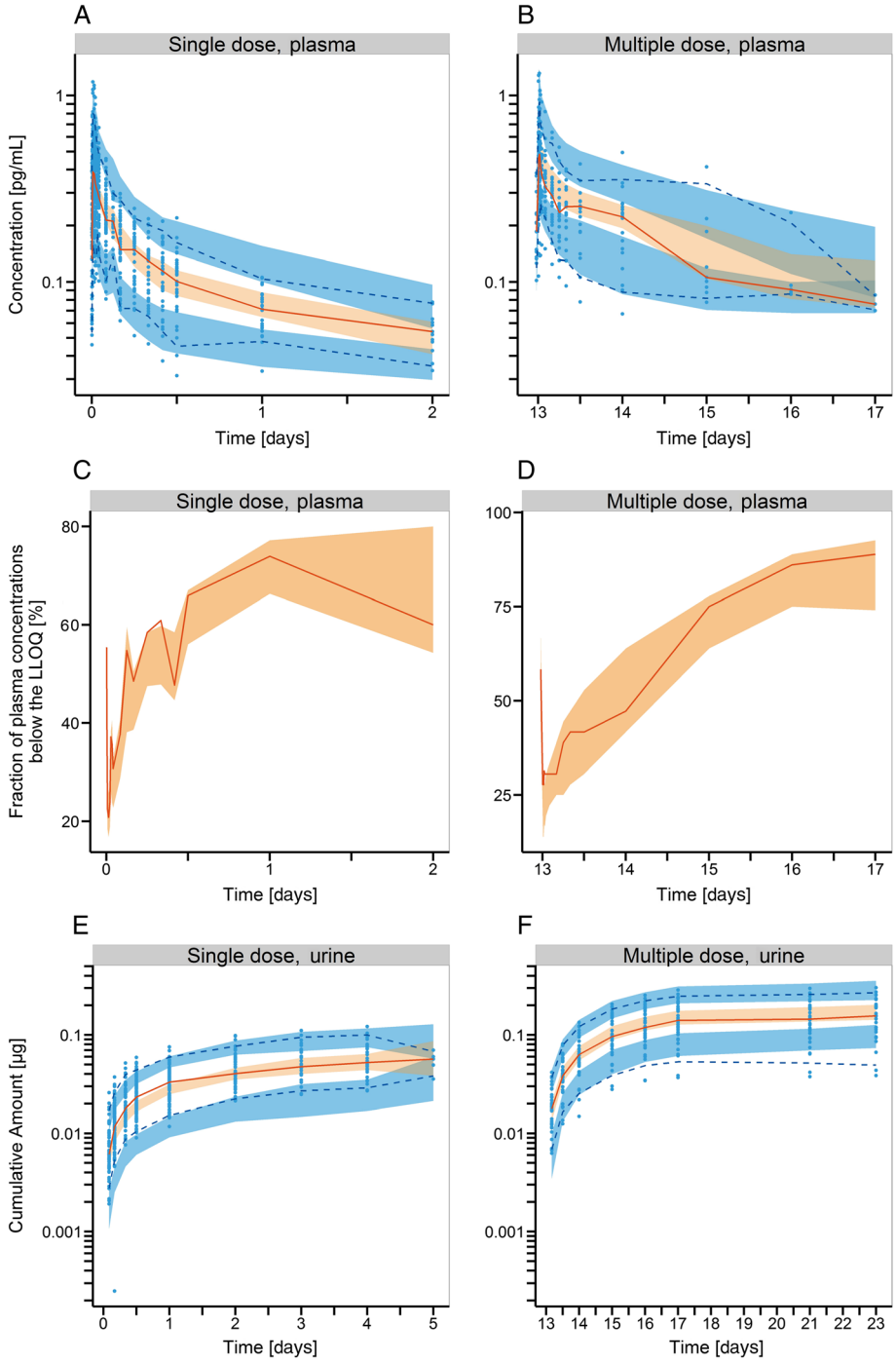

Figure 5

Dose-normalized visual predictive checks (VPC) to evaluate model performance. (A) Semi-logarithmic VPC for plasma concentrations after single-dose inhalation. (B) Semi-logarithmic VPC for plasma concentrations after multiple-dose inhalation (n_{dose} = 14). (C) VPC for plasma concentrations below the lower limit of quantification (LLOQ) after a single dose. (D) VPC for plasma concentrations below the LLOQ after multiple doses (n_{dose} = 14). (E) Semi-logarithmic VPC for the cumulative amount of olodaterol excreted into the urine after single-dose inhalation. (F) Semi-logarithmic VPC for the cumulative amount of olodaterol excreted into the urine after multiple-dose inhalation (n_{dose} = 14). The orange line represents the median of the observed data, the blue dashed lines represent the 5th and 95th percentiles of the observed data, the orange shaded area represents the 95% confidence interval around the median of the simulated data, the blue shaded area represents the 95% confidence interval around the 5th and 95th percentile of the simulated data and the blue points represent the measured concentrations

of smoking increasing the pulmonary absorption rate constant was demonstrated for inhaled insulin [31]. No physiologically plausible explanation for the impact of smoking on the slow absorption rate constant was found in literature. Simulations based on the best model provided a better quantitative assessment of the effect of

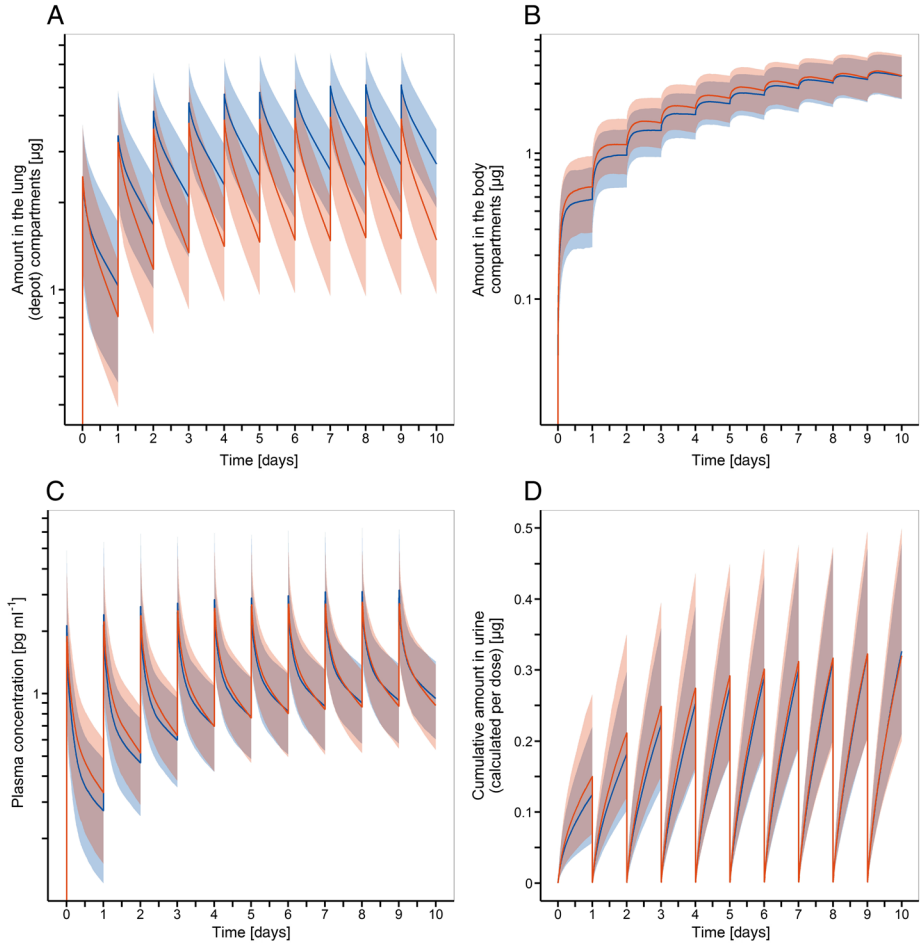

Figure 6

Simulations of different time profiles after inhalation of 5 µg olodaterol performed using the combined pharmacokinetic model. (A) Sum of drug amount in all depot (lung) compartments. (B) Sum of drug amount in all body compartments. (C) Plasma concentration–time profile. (D) Cumulative drug amount eliminated into the urine (calculated per dose). Blue profiles represent simulations performed in smokers, orange profiles represent simulations performed in nonsmokers, and blue and orange shaded areas represent 90% prediction intervals

smoking. Differences between smokers and nonsmokers were most pronounced in the unabsorbed drug amount; plasma concentration-time profiles were comparable between smokers and non-smokers (Figure 6), indicating that while differences in the pulmonary PK may exist they have a marginal influence on the plasma PK.

Another interesting finding of the covariate analysis was the increased pulmonary bioavailable fraction in females. Even though this covariate effect was removed during the backwards elimination procedure, it is in agreement with the literature suggesting a higher pulmonary particle/droplet deposition in females [32, 33]. The lack of statistical significance of this covariate may be due to the low number of females in the trial population (15 females/133 males). This covariate phenomenon might be an artifact of the stepwise model development approach. The effect of being female on systemic PK parameters could not be investigated during the first step of model development as no IV PK data were available from females. The same caveat would apply when expanding the current PK model to patients with asthma and COPD. For these patients, IV data are not available and, consequently, identifying potential differences in systemic drug disposition between patients and healthy volunteers is not feasible.

To date, different pulmonary absorption processes obtained by modelling have rarely been discussed. Based on *in vitro* and *ex vivo* experiments, it might be physiologically plausible to associate different absorption processes with different areas of the lung [34–36]. It has been suggested that drug deposited in the alveolar space is absorbed rapidly owing to a high perfusion of the alveolar space, a large absorption surface area (100 m^2), and a thin epithelial membrane [37]. On the other hand, drug deposited in the conducting airways might be absorbed slowly because of lower perfusion [38, 39] and thicker epithelial membranes [40]. A comparison of the simulated deposition patterns from a computational fluid dynamics model [41] with different absorbed proportions of inhaled olodaterol (PK model derived), did

not support this hypothesis. Simulated pulmonary deposition patterns after inhalation via the Respimat® inhaler indicated higher peripheral lung deposition (approximately 65% of the pulmonary bioavailable fraction deposited in airway generations 21 to alveoli [41]). It should be acknowledged that these simulation-based deposition patterns were predicted for tiotropium inhaled via the Respimat® inhaler. Though slight differences in drug deposition between the olodaterol formulation and the tiotropium formulation might exist, the qualitative deposition trend should be comparable. Hence, rapid absorption of a large proportion of drug is expected based on the mechanisms described above. This simulation-based assumption of a large rapidly absorbed proportion was inconsistent with the estimated large proportion (70%) that is slowly absorbed. Additional aspects might need consideration when it comes to understanding and subsequently predicting plasma or pulmonary absorption kinetics.

Various hypotheses have been discussed to explain the long-lasting activity of other inhaled β-sympathomimetic drugs. However, little evidence is available to support a pharmacokinetic-related reason for their long-lasting efficacy [21]. For salmeterol, possible explanations included the binding of the hydrophobic tail to a second location of the β_2-receptor ('off-site') or diffusion into the lipid membranes of airway smooth muscle cells [21]. These two hypotheses were rejected for inhaled olodaterol based on *in vitro* assays. It was demonstrated that a low receptor off-rate constant (0.039/h) reasonably explains the long-lasting efficacy [21]. In the present population PK analysis, it was additionally demonstrated that a long pulmonary residence time might contribute to the long effect duration.

A possible hypothesis to explain the different absorption half-lives of inhaled olodaterol, particularly the large proportion that is slowly absorbed, is lysosomal trapping in the lung. This microkinetic process has already been discussed for other drugs (e.g. antidepressants [42] or propranolol after IV administration [43]). These drugs [42] were basic compounds like olodaterol. Propranolol, for example, has a comparable chemical structure, similar physicochemical characteristics, and pK_a values to olodaterol (pK_a: 9.3, basic amine group, pK_a: 10.1 acidic phenolic group [21]). Basic molecules diffuse into the lysosomes of lung cells, such as macrophages or endothelial cells. Inside the lysosomes, lower pH results in protonation of basic molecules such as olodaterol, increasing the polarity of the molecules and reducing the backdiffusion of entrapped molecules from the lysosomes to the cytosol [44]. Such trapping could be a reasonable explanation for the observed high pulmonary residence time. It might also partly explain the discrepancy in the absorption kinetics and the suggested deposition patterns. Lysosomal trapping in the cells of the alveolar space might cause indirect olodaterol absorption from the alveolar space to the plasma (delayed by lysosomal trapping) parallel to direct absorption of drug from the alveolar space to the plasma. Further *in vitro* assays or physiologically-based PK modelling will be necessary to evaluate the impact of lysosomal trapping.

Irrespective of the underlying mechanism, the prolonged pulmonary residence time of inhaled olodaterol can be considered as an important kinetic aspect that might contribute to its long-lasting efficacy [21], and hence to the rationale of its once-daily regimen. As both inhaled tiotropium [14] and inhaled olodaterol exhibit comparable pulmonary absorption characteristics and are both administered using the Respimat®, they appear to be optimal partners for a combination product.

Conclusions

The pulmonary and systemic PK of inhaled olodaterol in healthy volunteers were investigated, applying a model-based approach. A key finding was the long pulmonary residence time of a high proportion of the pulmonary bioavailable fraction. Three distinct pulmonary absorption processes were identified which could not plausibly be matched with anatomical regions of the lung. Although lysosomal trapping in lung cells might be a plausible explanation, this hypothesis needs to be supported experimentally. Overall, the modelling and simulation approach provided new insights into the PK processes of inhaled olodaterol, and demonstrated that further research is needed to elucidate the mechanistic background and interpret the results of the modelling approach.

Competing Interests

All authors have completed the Unified Competing Interest form at http://www.icmje.org/coi_disclosure.pdf (available on request from the corresponding author) and declare that Benjamin Weber, Alexander Staab, Christina Kunz, and Stephan Formella are employees of Boehringer Ingelheim Pharma GmbH & Co. KG. The PhD project of Jens Markus Borghardt is funded by Boehringer Ingelheim GmbH & Co. KG. The authors declare no further conflict of interest.

REFERENCES

1 Patel JG, Nagar SP, Dalal AA. Indirect costs in chronic obstructive pulmonary disease: a review of the economic burden on employers and individuals in the United States. Int J Chron Obstruct Pulmon Dis 2014; 9: 289–300.

2 Global Initiative for Chronic Obstructive Lung Disease (GOLD). Global strategy for the diagnosis, management, and prevention of chronic obstructive pulmonary disease. 2015. Available from: http://www.goldcopd.org/

3 Gibb A, Yang LP. Olodaterol: first global approval. Drugs 2013; 73: 1841–6.

4 Olodaterol (Striverdi Respimat) for COPD. Med Lett Drugs Ther 2015; 57: 1–3.

5 Lipworth BJ. Systemic adverse effects of inhaled corticosteroid therapy: a systematic review and meta-analysis. Arch Intern Med 1999; 159: 941–55.

6 Kane C, O'Neil K, Conk M, Picha K. Inhalation delivery of protein therapeutics. Inflamm Allergy Drug Targets 2013; 12: 81–7.

7 Johnson EN, Druey KM. Heterotrimeric G protein signaling: role in asthma and allergic inflammation. J Allergy Clin Immunol 2002; 109: 592–602.

8 Hochhaus G, Mollmann H, Derendorf H, Gonzalez-Rothi RJ. Pharmacokinetic/pharmacodynamic aspects of aerosol therapy using glucocorticoids as a model. J Clin Pharmacol 1997; 37: 881–92.

9 Patton JS, Byron PR. Inhaling medicines: delivering drugs to the body through the lungs. Nat Rev Drug Discov 2007; 6: 67–74.

10 Ruge CA, Kirch J, Lehr CM. Pulmonary drug delivery: from generating aerosols to overcoming biological barriers-therapeutic possibilities and technological challenges. Lancet Respir Med 2013; 1: 402–13.

11 Borghardt JM, Weber B, Staab A, Kloft C. Pharmacometric models for characterizing the pharmacokinetics of orally inhaled drugs. AAPS J 2015; 17: 853–70.

12 Tronde A, Bosquillon C, Forbes B. The isolated perfused lung for drug absorption studies. In: Drug Absorption Studies: In Situ, In Vitro and In Silico Models, 1st edn, eds Ehrhardt C, Kim K-J. New York (NY), USA: Springer US, 2007; 135–63.

13 Bartels C, Looby M, Sechaud R, Kaiser G. Determination of the pharmacokinetics of glycopyrronium in the lung using a population pharmacokinetic modelling approach. Br J Clin Pharmacol 2013; 76: 868–79.

14 Parra-Guillen Z, Weber B, Sharma A, Freijer J, Retlich S, Borghardt JM, Troconiz IF. Population pharmacokinetic analysis of tiotropium in healthy volunteers after intravenous administration and inhalation. J Pharmacokinet Pharmacodyn 2014; 41: S54.

15 Borghardt JM, Weber B, Staab A, Kunz C, Schiewe J, Kloft C, eds. Expanding the Mechanistic Knowledge about Pulmonary Absorption processes using a Population Pharmacokinetic Model for Inhaled Olodaterol. Respiratory Drug Delivery. Fajardo, Puerto Rico: Davis Healthcare International Publishing, LLC., 2014.

16 US Department of Health and Human Services; Food and Drug Administration FDA. Guidance for industry: bioanalytical method validation, 2001; 1–22. Available from: http://www.fda.gov/downloads/Drugs/.../Guidances/ucm070107.pdf

17 Bonate PL. Nonlinear mixed effects models: theory. In: Pharmacokinetic–Pharmacodynamic Modeling and Simulation, 2nd edn, ed Bonate PL. New York (NY), USA: Springer, 2011; 233–301.

18 Lindbom L, Pihlgren P, Jonsson EN. PsN-toolkit – a collection of computer intensive statistical methods for non-linear mixed effect modeling using NONMEM. Comput Methods Programs Biomed 2005; 79: 241–57.

19 Keizer RJ, Karlsson MO, Hooker A. Modeling and simulation workbench for NONMEM: tutorial on pirana, PsN, and xpose. CPT Pharmacometrics Syst Pharmacol 2013; 2: e50.

20 Holford N, ed. The Visual Predictive Check – Superiority to Standard Diagnostic (Rorschach) Plots. PAGE Annual Meeting of the Population Approach Group in Europe, 2005; Pamplona, Spain.

21 Casarosa P, Kollak I, Kiechle T, Ostermann A, Schnapp A, Kiesling R, Pieper M, Sieger P, Gantner F. Functional and biochemical rationales for the 24-h-long duration of action of olodaterol. J Pharmacol Exp Ther 2011; 337: 600–9.

22 Patton JS, Fishburn CS, Weers JG. The lungs as a portal of entry for systemic drug delivery. Proc Am Thorac Soc 2004; 1: 338–44.

23 Dershwitz M, Walsh JL, Morishige RJ, Connors PM, Rubsamen RM, Shafer SL, Rosow CE. Pharmacokinetics and pharmacodynamics of inhaled versus intravenous morphine in healthy volunteers. Anesthesiology 2000; 93: 619–28.

24 Borgström L, Bengtsson T, Derom E, Pauwels R. Variability in lung deposition of inhaled drug, within and between asthmatic patients, with a pMDI and a dry powder inhaler, turbuhaler®. Int J Pharm 2000; 193: 227–30.

25 Brand P, Friemel I, Meyer T, Schulz H, Heyder J, Haubetainger K. Total deposition of therapeutic particles during spontaneous and controlled inhalations. J Pharm Sci 2000; 89: 724–31.

26 Boxenbaum H, Battle M. Effective half-life in clinical pharmacology. J Clin Pharmacol 1995; 35: 763–6.

27 Shaykhiev R, Otaki F, Bonsu P, Dang DT, Teater M, Strulovici-Barel Y, Salit J, Harvey BG, Crystal RG. Cigarette smoking reprograms apical junctional complex molecular architecture in the human airway epithelium *in vivo*. Cell Mol Life Sci 2011; 68: 877–92.

28 Jones JG, Minty BD, Lawler P, Hulands G, Crawley JC, Veall N. Increased alveolar epithelial permeability in cigarette smokers. Lancet 1980; 1: 66–8.

29 Li XY, Rahman I, Donaldson K, MacNee W. Mechanisms of cigarette smoke induced increased airspace permeability. Thorax 1996; 51: 465–71.

30 Minty BD, Jordan C, Jones JG. Rapid improvement in abnormal pulmonary epithelial permeability after stopping cigarettes. Br Med J (Clin Res Ed) 1981; 282: 1183–6.

31 Sakagami M. Insulin disposition in the lung following oral inhalation in humans: a meta-analysis of its pharmacokinetics. Clin Pharmacokinet 2004; 43: 539–52.

32 Kim CS, Hu SC. Regional deposition of inhaled particles in human comparison between men and women. J Appl Physiol 1998; 84: 1834–44.

33 Pichelin M, Caillibotte G, Katz I, Martonen T. Categorization of lung morphology based on FRC and height: computer simulations of aerosol deposition. Aerosol Sci Tech 2012; 46: 70–81.

34 French MC, Wishart GN. Isolated perfused rabbit lung as a model to study the absorption of organic aerosols. J Pharmacol Methods 1985; 13: 241–8.

35 Brown RA Jr, Schanker LS. Absorption of aerosolized drugs from the rat lung. Drug Metab Dispos 1983; 11: 355–60.

36 Schanker LS, Mitchell EW, Brown RA Jr Species comparison of drug absorption from the lung after aerosol inhalation or intratracheal injection. Drug Metab Dispos 1986; 14: 79–88.

37 Labiris NR, Dolovich MB. Pulmonary drug delivery. Part I: physiological factors affecting therapeutic effectiveness of aerosolized medications. Br J Clin Pharmacol 2003; 56: 588–99.

38 Upton RN, Doolette DJ. Kinetic aspects of drug disposition in the lungs. Clin Exp Pharmacol Physiol 1999; 26: 381–91.

39 Wanner A Clinical perspectives: role of the airway circulation in drug therapy. J Aerosol Med 1996; 9: 19–23.

40 International Commission on Radiological Protection. ICRP Publication 66 Human Respiratory Tract Model for Radiological Protection: New York, NY: Elsevier, 1994.

41 Ciciliani A-M, Wachtel H, Langguth P, eds. Comparing Respimat(R) Soft Mist(TM) Inhaler and DPI Aerosol Deposition by Combined *In Vitro* Measurements and CFD Simulations. Respiratory Drug Delivery. Fajardo, Puerto Rico: Davis Healthcare International Publishing, LLC., 2014.

42 Daniel WA, Wójcikowski J. Lysosomal trapping as an important mechanism involved in the cellular distribution of perazine and in pharmacokinetic interaction with antidepressants. Eur Neuropsychopharmacol 1999; 9: 483–91.

43 Dickens BF, Weglicki WB, Boehme PA, Mak TI. Antioxidant and lysosomotropic properties of acridine-propranolol: protection against oxidative endothelial cell injury. J Mol Cell Cardiol 2002; 34: 129–37.

44 MacIntyre AC, Cutler DJ. The potential role of lysosomes in tissue distribution of weak bases. Biopharm Drug Dispos 1988; 9: 513–26.

45 Cockcroft DW, Gault MH. Prediction of creatinine clearance from serum creatinine. Nephron 1976; 16: 31–41.

Supporting Information

Additional Supporting Information may be found in the online version of this article at the publisher's web-site:

Appendix S1
Extract of the NONMEM script of the population PK model with three parallel absorption processes

Figure S1
Graphical illustration of investigated pulmonary absorption models. Absorption model showing (top) different numbers of parallel absorption processes into the central body compartment; (lower left) direct pulmonary absorption into the peripheral body compartment; (lower middle) distribution into an additional hypothetical lung tissue compartment before absorption into the central body compartment; (lower right) transit absorption processes (k_{tr}: estimated as the same rate constant for two absorption processes, n_1 and n_2: estimated separately or predefined); top middle (green title box): best pharmacokinetic model with three parallel absorption processes. Blue boxes: systemic disposition compartments; green boxes: pulmonary absorption compartments.